ELSEVIER

Nuclear Instruments and Methods in Physics Research A 490 (2002) 251–262

NUCLEAR INSTRUMENTS & METHODS IN PHYSICS RESEARCH Section A

www.elsevier.com/locate/nima

Mass and charge identification of fragments detected with the Chimera Silicon–CsI(Tl) telescopes

N. Le Neindre[a], M. Alderighi[b], A. Anzalone[c], R. Barnà[d], M. Bartolucci[e], I. Berceanu[f], B. Borderie[g], R. Bougault[h], M. Bruno[a], G. Cardella[i], S. Cavallaro[c], M. D'Agostino[a,*], R. Dayras[j], E. De Filippo[i], D. De Pasquale[d], E. Geraci[c], F. Giustolisi[c], A. Grzeszczuk[k], P. Guazzoni[e], D. Guinet[l], M. Iacono-Manno[c], A. Italiano[d], S. Kowalski[k], A. Lanchais[a], G. Lanzanó[i], G. Lanzalone[i,g], S. Li[m], S. Lo Nigro[i], C. Maiolino[c], G. Manfredi[e], D. Moisa[f], A. Pagano[i], M. Papa[i], T. Paduszynski[k], M. Petrovici[f], E. Piasecki[n], S. Pirrone[i], G. Politi[i], A. Pop[f], F. Porto[c], M.F. Rivet[g], E. Rosato[o], S. Russo[e], S. Sambataro[i,✠], G. Sechi[b], V. Simion[f], M.L. Sperduto[c], J.C. Steckmeyer[h], C. Sutera[i], A. Trifirò[d], L. Tassan-Got[g], M. Trimarchi[d], G. Vannini[a], M. Vigilante[o], J. Wilczynski[p], H. Wu[n], Z. Xiao[n], L. Zetta[e], W. Zipper[l]

[a] *INFN and Dipartimento di Fisica Università di Bologna, Italy*
[b] *Istituto Fisica Cosmica, CNR and INFN Milano, Italy*
[c] *Laboratorio Nazionale del Sud INFN and Dipartimento di Fisica Università di Catania, Italy*
[d] *INFN and Dipartimento di Fisica Università di Messina, Italy*
[e] *INFN and Dipartimento di Fisica Università degli Studi, Milano, Italy*
[f] *Institute for Physics and Nuclear Engineering, Bucharest, Romania*
[g] *IPN, IN2P3-CNRS and Université Paris-Sud, Orsay, France*
[h] *LPC, ISMRA and Université de Caen, France*
[i] *INFN and Dipartimento di Fisica Università di Catania, Italy*
[j] *DAPNIA/SPhN - CEA Saclay, Gif sur Yvette Cedex, France*
[k] *Institute of Physics, University of Silesia, Katowice, Poland*
[l] *IPN, IN2P3-CNRS and Université Claude Bernard, Lyon, France*
[m] *Institute of Modern Physics, Lanzhou, China*
[n] *Institute of Experimental Physics, University of Warsaw, Poland*
[o] *INFN and Dipartimento di Fisica Università di Napoli, Italy*
[p] *Institute for Nuclear Studies, Otwock-Swierk, Poland*

Received 11 January 2002; received in revised form 26 March 2002; accepted 27 March 2002

*Corresponding author. Tel.: +39-51-209-1081; fax: +39-51-247-244.
E-mail addresses: dagostino@bo.infn.it (M. D'Agostino).
✠ Deceased.

PII: S0168-9002(02)01008-2

Abstract

Mass and charge identification of charged products detected with Silicon–CsI(Tl) telescopes of the Chimera apparatus are presented. An identification function, based on the Bethe–Bloch formula, is used to fit empirical correlations between ΔE and E ADC readings, in order to determine, event by event, the atomic and mass numbers of the detected charged reaction products prior to energy calibration.

PACS: 29.40.−n; 29.40.Mc; 29.40.Wk; 29.85.+c

Keywords: Radiation detectors; Scintillation detectors; Solid-state detectors; Computer data analysis

1. Introduction

In the last years, several new detectors for charged particle identification, with large solid angle coverage and high geometrical efficiency, have been built in order to investigate heavy-ions reactions at intermediate energies (10 A MeV to 1 A GeV) (see for instance [1]) [2].

These experimental devices give possibilities for simultaneous measurement of quantities related to energy, emission angle, atomic number and mass number of nearly all the charged reaction products. A very rich information can be extracted from these experimental studies, in particular, if the mass resolution of the apparatus is high. Indeed, isotope yields have proven to be a useful observable for studying the heavy-ion reaction mechanisms at intermediate and high energies [3]. Production yields of isotopically resolved nuclear particles and fragments can provide answers to the question of mutual stopping and subsequent equilibration of the collision partners. On the condition that equilibrium is reached, they allow to extract the corresponding thermodynamical variables, such as the temperature of the hot pieces of nuclear matter formed in the collision, their density and possibly the entropy.

The necessary step before the data analysis is the calibration of the measured signals. However, due to the fact that different detectors (ionization chambers, microstrips, semiconductors, scintillators) can be used, due to the rich variety of nuclear species produced in the reaction in a wide energy range and to the large number of telescopes covering the laboratory solid angle, this preliminary step is quite man-power and time consuming.

Another difficulty is that not necessarily all the detectors of a multi-modular ΔE–E telescope have a response linear in energy. The last generation 4π devices (see for instance [1]) [2] are multi-modular ΔE–E telescope systems, in which the residual-energy detectors are usually made of the CsI(Tl) scintillator. This choice is dictated by its relatively high stopping power, no limitation in geometrical shapes, negligible radiation damage, low cost, and good resolution. Since the light output of a scintillator depends both on the energy deposited in the crystal and on the atomic and mass numbers of the incident ion, the identification in mass and charge has to be done prior to energy calibration [4].

For the charge identification, semi-automatic [5] and automatic [6] techniques have been set in recent years, but no recent literature [7] is available for the mass identification, usually performed through graphical cuts [8] around each A-line in the ΔE–E scatter plot. This method, however, has the disadvantage that the number of contour lines that can be drawn is limited by the statistics and extrapolation to rare isotopes cannot be performed. Part of the physical information for isotopes populated with low statistics is then lost. In addition, measurements with neutron rich/poor beams and targets could lead to non-negligible shifts of the mass distributions with respect to stable isotopes, making difficult the A-labeling of the graphical cuts.

A fast and reliable method to assign the mass and charge of the detected ions is therefore highly desirable.

In this paper, we present a very effective mass and charge identification procedure which, as

compared with other methods, considerably saves time without loss of precision. The accuracy of the proposed method is checked by comparing the mass distributions obtained with this procedure with original mass distributions in model-generated samples.

We present here the application of our identification procedure to data collected in the first experiments performed by the Reverse collaboration with the forward part of the Chimera apparatus [9]. Mass and charge distributions obtained through more usual methods, like graphical cuts or particle identification functions, are compared with those obtained from our procedure.

2. Mass and charge particle identification function

We recall here the main principles leading to the used identification function. A more detailed description of the successive modifications of the Bethe–Bloch formula, to take care of the experimental distortions, can be found in Ref. [10].

Specific energy loss (dE/dx) of a charged particle in matter depends, as described by the classical Bethe–Bloch formula [11], on the mass A, charge Z and energy E of the incident ion and of the density and atomic number of the absorbing medium. For light ions with incident energy high enough to approximate the effective charge by the charge Z of the ion, the specific energy loss is

$$\frac{dE}{dX} = \frac{Z^2}{f(E/A)}. \tag{1}$$

Analytical reductions [10] of this expression lead to

$$\Delta E = [E^{\mu+1} + (\mu+1)Z^2A^{\mu}\Delta X]^{1/(\mu+1)} - E \tag{2}$$

in the case of particles detected in a ΔE–E telescope. ΔX is the thickness of the first detector, where the ion deposits an energy ΔE. In the second detector the ion is stopped and releases an energy E. To obtain Eq. (2) from Eq. (1) the hypothesis that $f(E/A)$ is a power-law

$$f(E/A) = (E/A)^{\mu} \tag{3}$$

with exponent $\mu \approx 1$ has been made [12].

Eq. (2) is the basic formula to build particle identification functions (*p.i.f.*) for charge identification. For instance, if we aim to identify the charge Z of a detected particle/fragment from the measured $\Delta E, E$ signals, we can calculate a not calibrated measure of Z (*p.i.f.*), which includes some unknown constants (like for instance the thickness of the ΔE detector and the exact relationship between the mass and the charge)

$$p.i.f. = [(\Delta E + E)^{\mu+1} - E^{\mu+1}]^{1/(\mu+2)} \tag{4}$$

with the assumption $A = 2Z$.

However, it is experimentally well known that it is quite difficult, by managing the only parameter μ, to find a unique *p.i.f.* able to linearize the ΔE–E correlation of each used telescope, in the whole range of residual energies and for a wide range of charges, as usually observed in heavy-ion reactions.

Modifications to Eq. (2) are therefore needed, since data deviate from the expected behaviour for several reasons:

- when the residual energy becomes low, the atomic charge is no longer equal to Z, especially for heavier elements;
- in experiments where the ion is stopped in a scintillator, the residual energy signal is not linear with the released energy. For a scintillator indeed, the light output response depends also on A and Z [4];
- when ΔE is measured with a Silicon detector, the pulse height defect influences the Silicon detector response for high Z-values.

To evaluate mass and charge, before energy calibration, an extension of Eq. (2), taking into account all the aforementioned problems has been proposed in Ref. [10]. This formula performs a decoupling of the ΔE–E correlation at low, intermediate and high energies, by introducing some free parameters and a phenomenological term, which takes care for the transition from low to high energies.

$$\Delta E = [(gE)^{\mu+\nu+1} + (\lambda Z^{\alpha}A^{\beta})^{\mu+\nu+1} + \xi Z^2A^{\mu}(gE)^{\nu}]^{1/(\mu+\nu+1)} - gE \tag{5}$$

where λ, μ, α, β, ν and ξ are free parameters, related to the characteristics and non-linear effects of the ΔE and E detectors. g accounts for the ratio of the electronic gains of the ΔE and E signals (QDC or ADC channels). Eq. (5) contains seven free parameters in case the subtraction of ΔE and E pedestals has already been performed.

Eq. (5) reduces to Eq. (2) if $g = 1$, $\nu = 0$, $\xi = 0$, $\alpha = 2/(\mu + 1)$, $\beta = \mu/(\mu + 1)$. In this case, the parameter λ results equal to $[(\mu + 1)\Delta X]^{1/(\mu+1)}$. Eq. (5) (see Ref. [10]) provides the same behaviour as Eq. (2) at vanishing and at high residual energies.

In Ref. [10] the application of Eq. (5) has been shown to be powerful for charge identification, in a wide range of products charge and for different ΔE–E types of telescopes. This has also been found to be valid in the case of new designed gas detectors as microstrips [13].

As far as the mass identification is concerned, Eq. (5) has been applied in Ref. [10] to a limited number of isotopes, since the data there presented were collected with devices providing mass resolution only for light fragments ($Z \leqslant 4$).

In the following, we will show the application of Eq. (5) to the Chimera [2] Si–CsI(Tl) telescopes, where the mass resolution is high up to $Z \leqslant 10$.

3. Identification procedure

The used identification procedure, consists of two steps:

- We sample on the ΔE–E scatter plot several points on the lines of well defined isotopes (He, Li, Be and B). In experiments, some isotopes can be easily recognized, due to their abundance (^{4}He, ^{7}Li, ^{11}B) or separation from other masses (^{7}Be, ^{9}Be).

  The charge, mass, ΔE and E signals of the sampled points are put in a table. A minimization routine[1] determines the parameters g, λ, α, β, μ, ν and ξ, giving the best agreement between the whole sample and the correlation provided for each A and Z by Eq. (5). The sum of the squared distances between the sampled and calculated values is minimized.

  This procedure is performed for each used telescope (688 for the case of the Reverse experiments) and a map is built containing the identification number of the telescope and its characteristic parameters λ, μ, α, β, ν, ξ and g.
- We perform the event by event identification.

  In each event, each detected particle/ion is identified in mass and charge by a two-step process, by minimizing the distance of the measured ΔE and E signals with respect to the values provided by Eq. (5) with the parameters g, λ, α, β, μ, ν and ξ read from the map built in the previous step. The two-dimensional vector $(\Delta E, E)$ is then replaced by the four-dimensional vector $(\Delta E, E, Z, A)$ for subsequent analyses.

  To identify mass and charge of the detected charged products a two-step process is needed, since Eq. (5) is not analytically solvable. The first step is to find the charge Z (simply assuming $A = 2Z$), by looking for the value of Z giving the shortest distance between the experimental ΔE and the energy loss given by Eq. (5) at the residual energy E. After the charge Z has been identified, the procedure is repeated, by solving Eq. (5) with respect to A.

This procedure is an improvement of the method developed in Ref. [5], extensively used in the Multics experiments for charge identification (see for instance Refs. [8,14,15]) when cocktail beams were not available.

The improvement consists not only in the simultaneous event by event mass and charge identification, but mainly in the use of the analytical form of the ΔE–E correlation Eq. (5) together with the map of parameters characterizing the individual response of each telescope. Deviations of the Silicon detector thickness with respect to the values provided by the factory as well as intrinsic scintillation efficiency of the CsI(Tl) crystals are taken into account by the map parameters. Consequently, the interpolation or extrapolation to values of A and Z not sampled

[1] MINUIT D506 routine from the CERN Program Library.

or emitted with low probability should be under control.

This will be verified in the following sections.

4. Check of the procedure through model events

As an example of the identification procedure, we first show the application of our method to a set of ideal events, where not only the signals ΔE and E are known, but also the mass number A and the charge number Z. The comparison between the original values of (Z, A) and the reconstructed ones allows to evaluate the capability and the limits of the procedure.

The *ideal* events used to check the identification function (5) are generated by the statistical multifragmentation model SMM [16]. This model reproduces in great detail static and dynamic experimental observables, like charge, mass and kinetic energy distributions [8,14,17]. We analyze here events of the decay of a Au source, with excitation energy in the range 1–8 A MeV and density one-third of the normal density [15].

For each event, from the mass number, charge number and kinetic energy of the charged decay products we compute their ΔE (energy loss in a 280 μm Silicon detector) and the residual energy E.

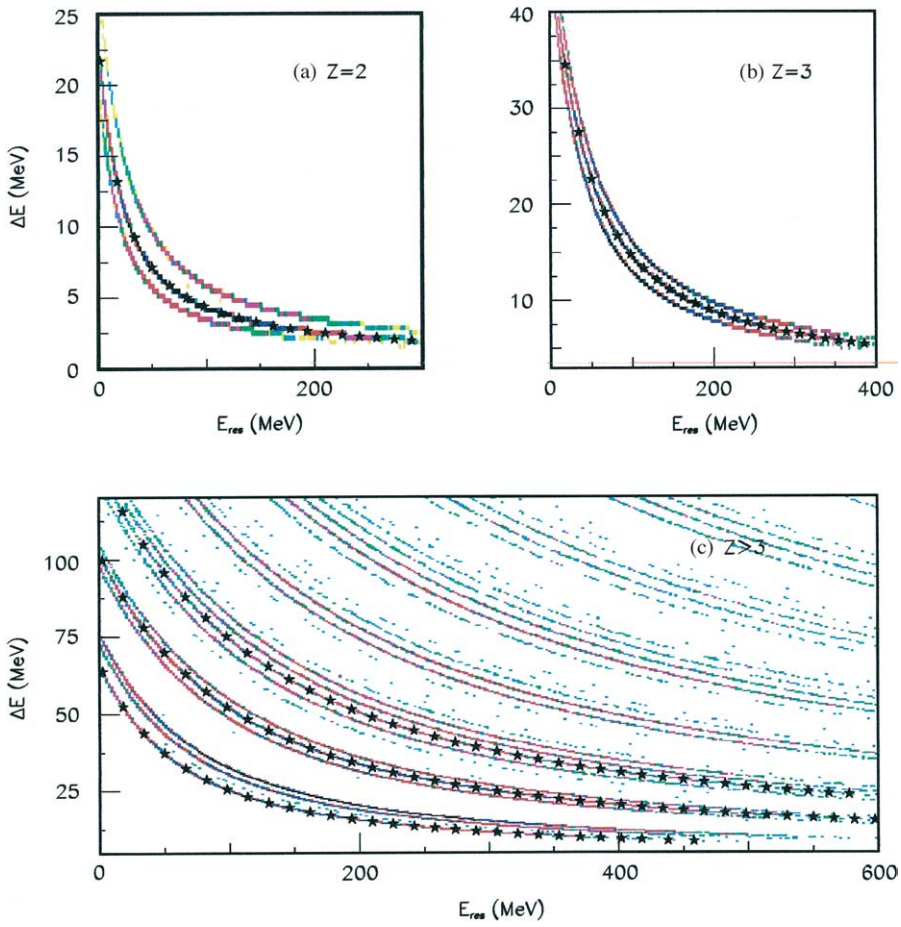

Fig. 1. Model events: ΔE–E plots (colors from yellow to black follow a logarithmic scale) for ions passing through a 280 μm Silicon detectors. Stars at $Z = 2, A = 4$ (panel a), $Z = 3, A = 7$ (panel b), $Z = 4, A = 7$, $Z = 5, A = 11$ and $Z = 6, A = 12$ (panel c) are the sampled points used for the fitting procedure.

In Fig. 1 we show the ΔE–E plots for $Z = 2$, $Z = 3$ and $Z \geqslant 4$ (panels a, b, and c, respectively). The stars in Fig. 1 represent the sampled points, used to calculate the parameters of Eq. (5). From the seven parameters, fit of the sample (165 points, step 16 MeV in the residual energy), we obtain a description of the ΔE–E correlation under study, characterized by an average distance between the sampled points and the values calculated through Eq. (5) of ≈ 0.1 MeV.

Since we are dealing with energies, the ratio of the gains g results ≈ 1. The parameter v results nearly zero and α and β satisfy the relationships $\alpha = 2/(\mu + 1)$, and $\beta = \mu/(\mu + 1)$, as expected for an ideal detector.

We compare now the original mass distribution of the model, for isotopes not used for the fit, with the one calibrated through our identification procedure. We want indeed to estimate how far we can extrapolate above the highest charge contained in the sample ($Z = 6$), still having a reliable reproduction of the A-distributions.

In Fig. 2 we compare the A-distributions for charges not included in the fit: $Z = 1$ and 8–12. Histograms are the original yields of the model, symbols are values obtained from Eq. (5). For $Z = 1$, 8 and 9 the calculated yields are in perfect agreement with the model. For $Z \geqslant 10$ discrepancies appear between original and reconstructed mass yields. For instance for $Z = 10, A = 20$ and for $Z = 12, A = 26$ the deviation is about 15%.

As far as the charge identification is concerned, over the whole set of considered charged products ($1 \leqslant Z \leqslant 12$), Eq. (5) has been found to fail in the charge determination (by one charge unit) with a probability smaller than 3×10^{-5}. We have also found that, when interpolating between sampled ΔE–E lines, the calculated mass yields are in perfect agreement with the model ones.

The results shown in Figs. 1 and 2 have been obtained for an ideal telescope, with perfect resolution. Now we consider the modifications induced by finite energy resolution. We perform this check in the case of an energy resolution 2% for the ΔE detector and 4% for the stopping detector (much worse than those observed for the Chimera detectors). The chosen values of the resolutions still allow to resolve the isotope lines.

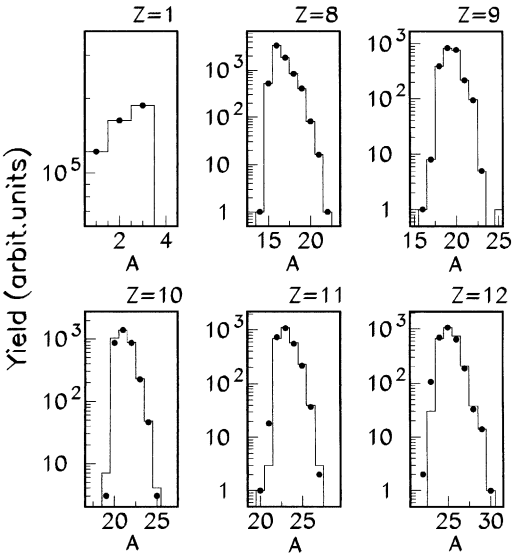

Fig. 2. Model events: Isotopic distributions obtained from the extrapolation of Eq. (5) to isotopes not used in the fit. Lines represent the model A-distributions, full symbols the values calculated from Eq. (5).

By repeating the analysis shown in Fig. 2, we have found the same results as before for charge determination and mass interpolation. As far as mass identification for charges above the highest charge contained in the sample, the agreement between true and calculated mass yields slightly worsens with respect to the case of a "perfect" detector. Indeed for $Z = 9$ ($A = 20$) calculated values differ by 4% with respect to the original ones, for $Z = 10, A = 20$ and for $Z = 12, A = 26$ the deviation is about 25%.

These results establish the confidence level for mass identification of charges not included in the sampled set. We conclude that the proposed procedure is suitable to reliably extrapolate masses up to three charges above the highest charge contained in the sample, even when considering ΔE–E correlations spread by the detector resolution.

5. Experimental results

In this Section, we show the results of the identification procedure applied to experimental

data. The data have been collected, for the reactions $^{124}Sn + {}^{64}Ni$, $^{112}Sn + {}^{58}Ni$ and $^{124}Sn + {}^{27}Al$ at 35 A MeV incident energy, in experiments performed at the Superconducting Cyclotron of LNS (Catania) by the Reverse collaboration [18]. The forward part ($\theta_{lab} \leqslant 30^{\circ}$) of Chimera array was used for the experiments. In this configuration, 688 telescopes made of ΔE Silicon detectors 200–300 μm thick (depending on θ_{lab}) and CsI (Tl) stopping detectors were used.

The energy signal of the silicon detector was obtained by a standard spectroscopic line, made by a fast low noise charge sensitive preamplifier (PAC), followed by a main spectroscopic amplifier (~ 0.75 μs shaping time).

The light output of the crystal was collected by a 20×20 mm^2 photodiode coupled with a low noise 45 mV/MeV PAC. The PAC output signal was shaped by a spectroscopic amplifier (2 μs shaping time) and the shaped signal was stretched in order to avoid any time jitter in the digital conversion performed by a 64 channels VME single gate QDC.

The energy resolutions of the silicon detectors and the CsI(Tl) crystals were quoted by measuring the elastic scattering of different ion beams, delivered by the Tandem and the Cyclotron accelerators of the LNS in Catania, impinging on a thin (~ 100 μg/cm^2) Au target. The typical energy resolution of a Chimera telescope resulted

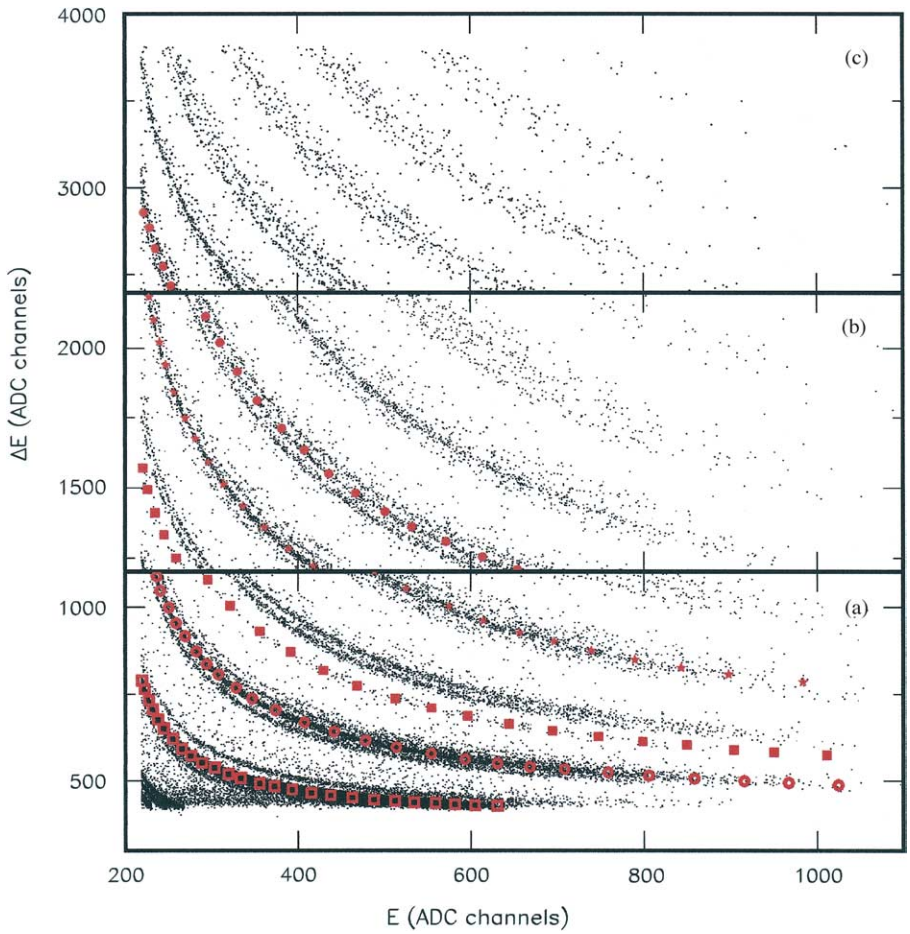

Fig. 3. Experimental ΔE–E scatter plot for a Chimera telescope at $\theta_{lab} = 21^{\circ}$. Red symbols are the sampled points used in the fitting procedure: ^{4}He (open squares), ^{7}Li (open circles), ^{7}Be (full squares), ^{11}B (stars), ^{13}C (full points).

$<1\%$ for the Silicon detector and about 2% for the CsI(Tl). As an example, with beams of ^{58}Ni at 15.5 A MeV the energy resolution (FWHM) was 0.5% for the Silicon detector and 1.5% for the crystal, using the lowest value of the gain ($g = 1$ V/V) of the main amplifier. The energy resolution of silicon detectors was also measured by collecting α-particles of a standard three peaks radioactive source. Typical energy resolutions were ~ 70 keV with $g = 8$ V/V and ~ 200 keV with $g = 2$ V/V. In order to reduce possible distortions of the electric field, the polarization bias of the Silicon detectors was increased by 30% with respect to the nominal one. As a global result, in 95% of the ΔE–E matrices a good identification of the atomic number (up to a charge $Z = 50$ for the most forward angle), was obtained in the full dynamical range of the experiment (see Fig. 6). Finally, in the high gain conversion range of the QDC [2], corresponding to a dynamical range of about 120 MeV with a PAC sensitivity of 4.5 mV/MeV and $g = 2$ V/V, a good identification of isotopes from charge $Z = 3$ up charge $Z = 8$ was clearly achieved (see Fig. 3).

5.1. Mass identification

We start the analysis, by sampling a set of $(\Delta E, E)$ points (see Fig. 3). The isotopes chosen to build the sample set are ^{4}He, ^{7}Li, ^{7}Be, ^{11}B, ^{13}C.

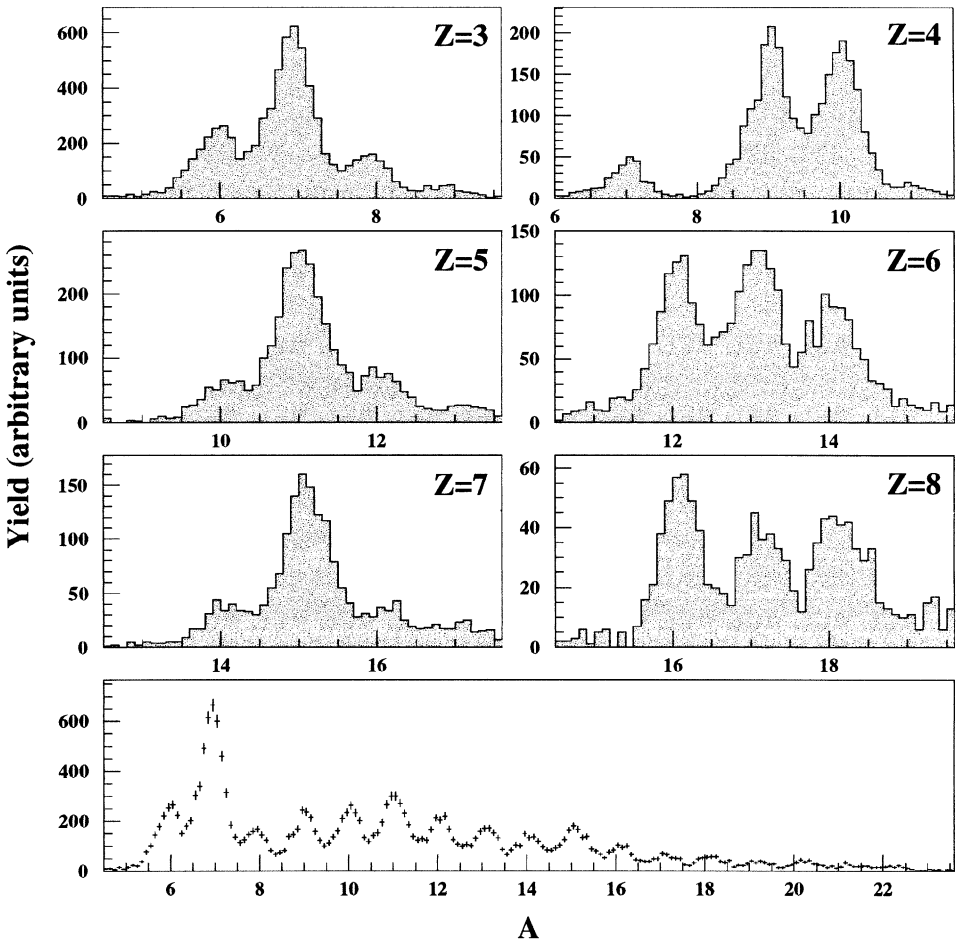

Fig. 4. Experimental isotopic distributions obtained for charges 3–8. The bottom histogram represents the mass distribution for charges 3–10.

As a second step we fit the data (122 points) with Eq. (5), with nine free parameters (both ΔE and E are QDC channels, the pedestals have not been subtracted).

Table 1
Comparison of the isotope yields obtained from graphical cuts and from Eq. (5)

Isotope	Graphical cuts	Eq. (5)
^{6}Li	864	865
^{7}Li	1950	1948
^{8}Li	547	520
^{7}Be	264	244
^{9}Be	1114	1080
^{10}Be	1173	1109
^{10}B	350	354
^{11}B	1673	1600
^{12}B	494	519
^{12}C	745	707
^{13}C	860	858
^{14}C	616	579

The resulting total

$$\chi^2 = \frac{1}{\text{d.o.f.}} \sum \frac{(\Delta E - \Delta E_{\text{calc}})^2}{\text{errors}^2}$$

is 2.3 (d.o.f. stands here for the degrees of freedom, number of the sampled points minus the number of free parameters). The errors on the experimental sampled points (channels) have been estimated to be about 10 channels, by sampling several times the same ΔE–E experimental matrix. All the sampled isotopes give comparable partial contributions to the total χ^2.

Finally, the event by event identification was performed. The resulting isotopic distribution for individual charges from $Z = 3$ to 8 is shown in Fig. 4. In the same figure is also reported the mass spectrum, obtained for charges from 3 to 10 (from ^{6}Li to ^{23}Ne, respectively). The quality of the mass identification obtained from our procedure is remarkable. Indeed, the *peak over noise* ratio of the mass distribution, even when integrated over

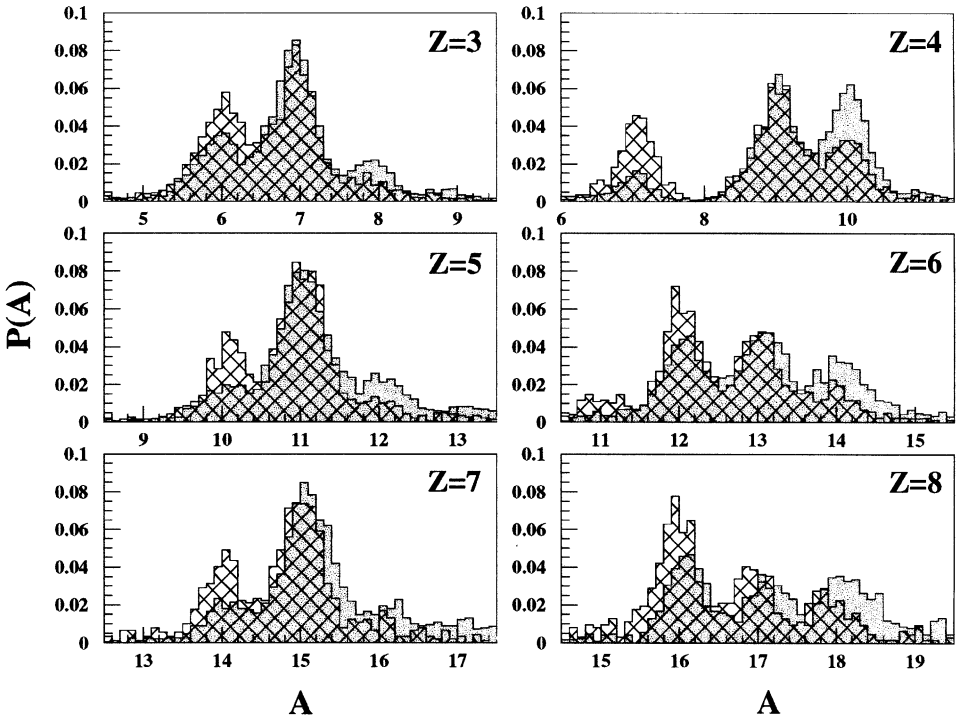

Fig. 5. Experimental isotopic distributions obtained for charges 3–8. The grey histogram refers to the reaction ^{124}Sn + ^{64}Ni and the hatched one to the reaction ^{112}Sn + ^{58}Ni. The histograms have been normalized to the total area for each charge.

eight charges, remains similar to the one obtained by looking at separated charges.

We have checked the accuracy of our procedure, by comparing the yields obtained from Eq. (5) with those obtained with graphical cuts performed on the A-lines, in the regions where these lines are clearly distinguishable. From Table 1 it is evident that all the mass yields are in agreement within the statistical uncertainties. In addition, the yields obtained from Eq. (5) resulted in very good agreement with gaussian integrals of the isotope distribution of Fig. 4.

We want to remark on another advantage of our identification procedure with respect to graphical cuts.

The a priori A-labeling of the observed ΔE–E correlations (see Fig. 3) in the region of heavy ($Z > 4$) isotopes could be disputable, in absence of reference beams sent on the detectors and/or before energy calibration and comparisons to energy-loss calculation. Indeed, noticeable shifts of the mass distributions with respect to stable isotopes are expected [19] in experiments running with neutron rich/poor beams and targets (as in the case of Reverse experiments).

In the case of the adopted procedure quantitative *reliability* tests can be performed by checking the partial contribution of the sampled isotopes to the total χ^2. For instance, if the fit of the sampled points (shown in Fig. 3) is performed, by assuming the mass of the sampled $Z = 6$ isotope as $A = 12$ (instead of 13), the corresponding partial contribution rises to a value about 25 (instead of ~ 2).

As an example of the rich variety of isotopes produced in reactions with neutron rich/poor projectile and targets, we compare in Fig. 5 the mass distributions measured for the reactions $^{124}\mathrm{Sn} + {}^{64}\mathrm{Ni}$ and $^{112}\mathrm{Sn} + {}^{58}\mathrm{Ni}$ at 35 A MeV (respectively $N/Z = 1.41, 1.18$). The isospin of the entrance channel reflects on large shifts of the mass

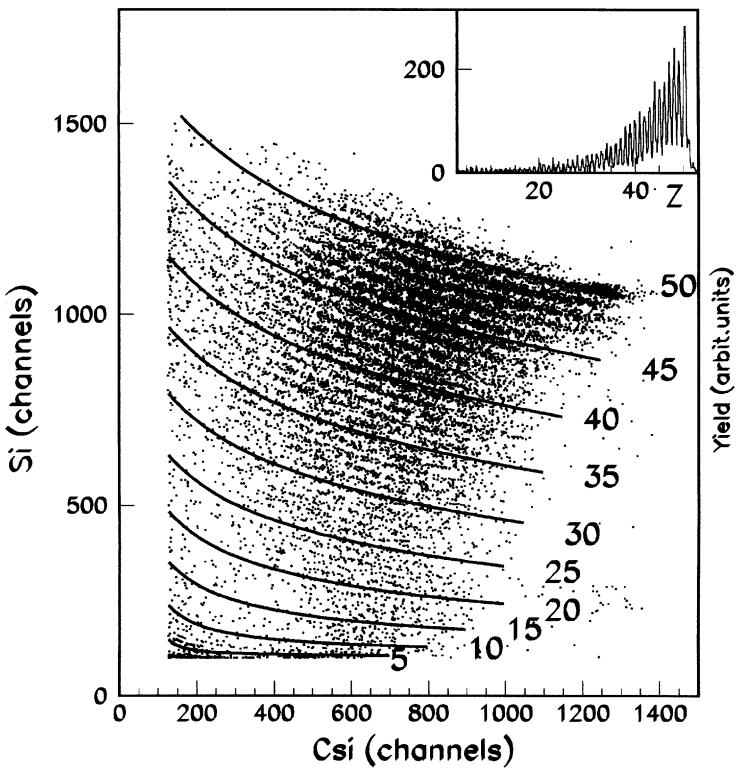

Fig. 6. Experimental ΔE–E scatter plot for a Chimera telescope at $\theta_{\mathrm{lab}} = 1^{\circ}$. Lines show the values calculated from Eq. (5). The insert panel shows the charge identification obtained with the p.i.f. method (see text).

distributions. Neutron rich systems enhance the production of neutron rich isotopes, as expected from theoretical calculations [19], mainly in the even charge isotopes. Study of heavy-ion reaction mechanisms are therefore feasible, to provide information on thermodynamical variables of equilibrated hot sources formed in the collision, such as their temperature and density.

5.2. Charge identification

As another example of the identification method we show in the following the application of our procedure to identify the charge of fragments collected by a forward detector ($\theta_{lab} = 1^\circ$) of the Chimera array.

Also in this case we sample a set of $(\Delta E, E)$ points. We build a set of sampled points for $2 \leqslant Z \leqslant 9$, $Z = 15$, 20, 30, 40 and 50, and we fit this sample with Eq. (5). We obtain a set of parameters, associated to the examined detector, reproducing the sampled points with a

$$\chi^2 = \frac{1}{\text{d.o.f.}} \sum \frac{(\Delta E - \Delta E_{\text{calc}})^2}{\text{errors}^2}$$

equal to 0.45. All the observed ΔE–E Z-lines are well reproduced up to the whole $Z = 50$ line (see Fig. 6).

In Fig. 7 we compare the corresponding charge distribution with the one obtained by a particle identification function (Eq. (4)) (upper insert panel of Fig. 6). The overall agreement is very good. Some disagreement between the two distributions is present for low values of atomic numbers, which suffer of poor statistics and at very high values of the charge number, for which the determination of the charge through the p.i.f results less precise than at intermediate Z-values. Indeed, the *peak over noise* ratio ranges from a value larger than 5 (up to charges $\simeq 30$) to ~ 4 at $Z = 50$. As a consequence, the contamination among adjacent charges goes from 2% to about 4%.

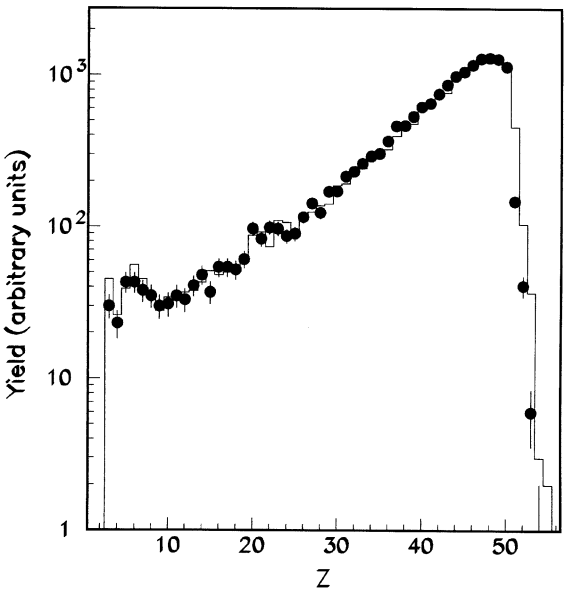

Fig. 7. Experimental charge distribution for the ΔE–E matrix of Fig. 5. Symbols show the values calculated from Eq. (5). Lines show the yields calculated through a particle identification function (see text).

6. Conclusions

We have presented a semi-automatic Z and A identification procedure, tested through the analysis of model events with known distributions. Very good agreement was obtained.

The experimental results have been verified by comparing the obtained A and Z distributions with those resulting from standard methods (graphical cuts or particle identification functions). The results of these comparison resulted quite satisfactory, and the uncertainties on the charge and mass identification are clearly improved.

The advantages of the procedure may therefore be summarized as follows:

- Beams of known mass, charge and energy are not needed for the charge and mass identification of charged products, detected with ΔE–E telescopes with good energy resolution.
- If mass is not resolved, Z-identification is still possible by substituting in Eq. (5) A with $2Z$ or with other parameterizations commonly used in experiments [20,21].
- The accuracy of the mass identification is very high, at least comparable in precision with the graphical cuts in ΔE–E matrices, but clearly more powerful because our procedure saves a

lot of time, especially in experiments involving many telescopes.

- The use of a map of identification parameters, taking into account the response of each telescope, makes possible the extrapolation to A-regions where graphical cuts are not easy to make, due to low statistics.
- Possible drifts of the electronic circuits can be diagnosed by controlling the constancy of the parameters of the map during the sequence of runs throughout the whole experiment.
- The method ensures relatively fast, standardized and reliable mass and charge identification for multi-telescope systems.

Acknowledgements

The authors wish to thank R. Bassini, C. Boiano, C. Cali', V. Campagna, R. Cavaletti, O. Conti, M. D'Andrea, F. Fichera, N. Giudice, A. Grimaldi, N. Guardone, S. Hong, P. Litrico, G. Marchetta, S. Marino, D. Nicotra, G. Peirong, C. Rapicavoli, G. Rizza, G. Sacca', S. Salomone, S. Urso, for the technical support during the experiment. The authors are also grateful to L. Calabretta and D. Rifuggiato for the assistance in delivering beams of very good timing quality.

This work was supported in part by the Italian Ministry of University and Scientific Research under grants Cofin99 and by NATO grants PST/CLG 976861.

References

[1] U. Lynen, et al., Gesellschaft für Schwerionenforschung Report No. GSI-02-89;
R.T. de Souza, et al., Nucl. Instr. and Meth. A 295 (1990) 109;
I. Iori, et al., Nucl. Instr. and Meth. A 325 (1993) 458;
J. Pouthas, et al., Nucl. Instr. and Meth. A 357 (1995) 418.

[2] S. Aiello, et al., Nucl. Phys. A 583 (1995) 461;
S. Aiello, et al., Nucl. Instr. and Meth. A 369 (1996) 50;
S. Aiello, et al., Nucl. Instr. and Meth. A 400 (1997) 469;
S. Aiello, et al., IEEE Trans. Nucl. Sci. NS-47 (2) (2000) 114.

[3] J. Pochodzalla, W. Trautmann, nucl-ex/0009016, and Isospin Physics in Heavy-Ion Collisions at Intermediate Energies, in: Bao-An Li, W.U. Schröder (Eds.), Nova Science Publisher, New York, 2001, p. 451.

[4] P.F. Mastinu, P.M. Milazzo, M. Bruno, M. D'Agostino, L. Manduci, Nucl. Instr. and Meth. A 338 (1994) 419;
P.F. Mastinu, P.M. Milazzo, M. Bruno, M. D'Agostino, L. Manduci, Erratum: Nucl. Instr. and Meth. A 343 (1994) 663.

[5] P.F. Mastinu, P.M. Milazzo, M. Bruno, M. D'Agostino, Nucl. Instr. and Meth. A 371 (1996) 510.

[6] M. Alderighi, et al., Comput. Phys. Commun. 140 (2001) 13;
M. Alderighi, et al., IEEE Trans. Nucl. Sci. NS-48 (2001) 385.

[7] T. Shimoda, et al., Nucl. Instr. and Meth. A 165 (1979) 261.

[8] P.M. Milazzo, et al., Phys. Rev. C 58 (1998) 953.

[9] A. Pagano, et al., Nucl. Phys. A 681 (2001) 331c.

[10] L. Tassan-Got, arXiv:nucl-ex/0103004, Nucl. Phys. B (2002), in press.

[11] H.A. Bethe, Ann. Phys. 5 (1930) 325.

[12] F.S. Goulding, B.G. Harvey, Ann. Rev. Nucl. Sci. 25 (1975) 167.

[13] F. Gramegna, et al., Nucl. Instr. and Meth. A 389 (1997) 474.

[14] M. D'Agostino, et al., Phys. Lett. B 371 (1996) 175.

[15] M. D'Agostino, et al., Nucl. Phys. A 650 (1999) 329.

[16] J. Bondorf, A.S. Botvina, A.S. Iljinov, I.N. Mishustin, K. Sneppen, Phys. Rep. 257 (1995) 133.

[17] R. Bougault, et al., in: I. Iori, XXXV International Winter Meeting on Nuclear Physics, Bormio, Italy, February 1997, Ric. Sc and E.P., Vol. 110, 1997.

[18] E. Geraci, et al., in: G. Bonsignori, M. Bruno, A. Ventura, D. Vretenar (Eds.), Nucleus–Nucleus Collisions, World Scientific, Singapore, 2000, p. 409;
G. Politi, et al., in: G. Bonsignori, M. Bruno, A. Ventura, D. Vretenar (Eds.), Nucleus–Nucleus Collisions, World Scientific, Singapore, 2000, p. 413.

[19] M. Di Toro, et al., Nucl. Phys. A 681 (2001) 426c.

[20] R.J. Charity, et al., Phys. Rev. Lett. 56 (1986) 1354.

[21] K. Sümmerer, W. Bruüchle, D.J. Morrissey, M. Schädel, B. Szweryn, Yang Weifan, Phys. Rev. C 42 (1990) 2546.